mm data obtained in May 1992 with use of four VLBA antennas. Their data are in general agreement with our results. Their best fit to a circular Gaussian model has a diameter of 0.75 mas, which is identical to our result, and their B1 component is consistent with our closure-amplitude fit. Both observations are dominated by the east-west structure owing to the limited range of baseline projections. Krichbaum *et al.* suggest the presence of one or more additional faint components with 0.2 to 0.4 Jy for which we have no evidence. The total flux density of the source at the epoch of their observations was 0.8 Jy less than that found during ours, and this could result in some differences owing to limited dynamic range. New observations with the full VLBA made under good weather conditions over multiple epochs are needed.

A long-standing alternative to the scattering interpretation for the observed wavelength-dependent brightness distribution is a nonuniform thermal or synchrotron source (*14*). Although such models could match the observations, extreme parameters are required, and, most importantly, the observed scattering of the OH masers within 15 arc min of Sgr A* would need to be coincidental. Melia (*3*) has explored further a nonuniform source model using the context of accretion onto a massive black hole from the winds blown out of the IRS 16 complex. He assumed that current size estimates are dominated by scattering and makes predictions about the contribution of the intrinsic source distribution to the apparent size as a function of wavelength. This work makes a number of critical assumptions to allow estimation of the spectrum from radio waves to x-rays for a range of central masses. On the basis of calculations that have been used to develop this black hole model (*15*), our upper limit to the intrinsic size of 3.3 AU corresponds to an upper limit to the mass of the black hole at the galactic center of 1.5×10^6 solar masses. This is comparable to estimates based on other lines of evidence (*16*). The radio source luminosity of Sgr A* is about 10^{34} erg s^{-1} for an isotropic spectrum of radiation extending to 100 GHz (*17*). The small size and large radio luminosity of Sgr A* in combination with its low peculiar velocity (*18*) and its central location in the 3.8–arc sec (0.15-pc), dense stellar cluster (*1*) are all strong indicators that the underlying body of Sgr A* is a massive black hole.

REFERENCES AND NOTES

1. A. Eckart, R. Genzel, R. Hoffman, *Astrophys. J.* **407**, L77 (1993).
2. R. Sanders, *Nature* **359**, 131 (1992).
3. F. Melia, *Astrophys. J.* **387**, L25 (1992).
4. L. Ozernoi, *Ann. N.Y. Acad. Sci.* **688**, 596 (1993).
5. R. Sunyaev *et al.*, *Sov. Astron. Lett.* **17**, 42 (1991); M. R. Rosa, H. Zinnecker, A. Moneti, *Astron. Astrophys.* **257**, 515 (1991); A. Eckart *et al.*, *Nature* **355**, 526 (1992).
6. K. Y. Lo *et al.*, *Nature* **315**, 124 (1985); D. L. Jauncey *et al.*, *Astron. J.* **98**, 44 (1989); J. M. Marcaide *et al.*, *Astron. Astrophys.* **258**, 295 (1992); K. Y. Lo *et al.*, *Nature* **362**, 38 (1993).
7. J. Armstrong, *Astrophys. J.* **358**, 685 (1990); J. Higdon, *ibid.* **285**, 109 (1984); *ibid.* **309**, 342 (1986).
8. D. C. Backer, in *Radio Wave Scattering in the Interstellar Medium*, J. Cordes, B. Rickett, D. Backer, Eds. (Conference Proceeding 174, American Institute of Physics, New York, 1988), p. 111.
9. H. J. van Langevelde, D. A. Frail, J. M. Cordes, P. J. Diamond, *Astrophys. J.* **396**, 686 (1992).
10. J. Goodman and R. Narayan, *Mon. Not. R. Astron. Soc.* **238**, 995 (1989).
11. S. Spangler and C. Gwinn, *Astrophys. J.* **353**, L29 (1990).
12. A. C. S. Readhead *et al.*, *Nature* **285**, 137 (1980).
13. T. Krichbaum *et al.*, *Astron. Astrophys.* **274**, L37 (1993).
14. G. de Bruyn, *ibid.* **52**, 439 (1976); R. L. Brown, K. Y. Lo, K. J. Johnston, *Astron. J.* **83**, 1594 (1978); S. P. Reynolds and C. F. McKee, *Astrophys. J.* **239**, 893 (1980).
15. F. Melia, J. R. Jokipii, A. Narayanan, *Astrophys. J.* **395**, L87 (1992); F. Melia (personal communication) has recalculated these results with an emissivity formula that corrects an error in this reference and in (*3*). The mass estimates in this paper are from the corrected results.
16. R. Genzel, D. Hollenbach, C. H. Townes, *Rep. Prog. Phys.*, in press.
17. R. Zylka, P. G. Mezger, H. Lesch, *Astron. Astrophys.* **261**, 119 (1992); M. C. H. Wright and D. C. Backer, *Astrophys. J.*, in press.
18. D. C. Backer and R. A. Sramek, in *The Galactic Center*, D. C. Backer, Ed. (Conference Proceeding 155, American Institute of Physics, New York, 1987), p. 163.

19. The VLBA is being constructed by the National Radio Astronomy Observatory (NRAO). The NRAO is operated by Associated Universities, Inc., under contract from the National Science Foundation (NSF). Part of this work was done while K.I.K. was a Sherman Fairchild Distinguished Visitor at Caltech, supported by the NSF (AST-911700), and J.M.M. was a Humboldt Fellow at the Max Planck Institute for Extraterrestrial Physics. The effort by D.C.B. is supported by the NSF (AST-9003404).

2 June 1993; accepted 15 October 1993

Photoactivated Conformational Changes in Rhodopsin: A Time-Resolved Spin Label Study

Zohreh Toossi Farahbakhsh, Kálmán Hideg, Wayne L. Hubbell*

Rhodopsin has been selectively spin-labeled near the cytoplasmic termini of helices C and G. Photoactivation with a light flash induces an electron paramagnetic resonance spectral change in the millisecond time domain, coincident with the appearance of the active metarhodopsin II intermediate. The spectral change is consistent with a small movement near the cytoplasmic termination of the C helix and reverses upon formation of the MIII state. These results provide an important link between the optical changes associated with the retinal chromophore and protein conformational states.

Rhodopsin is a member of the receptor family linked to G proteins (heterotrimeric guanosine triphosphate–binding proteins) and is one of the most extensively studied because of its natural abundance in the retina. The activation of receptors in this family presumably leads to a conformational change that presents new topological features recognized by a G protein. In rhodopsin, light absorption initiates a cascade of events involving discrete intermediates, each defined by an optical absorption maximum arising from the retinal chromophore (*1*). The relation of the optical changes to structural changes in the protein remains uncertain, but it appears that receptor activation is closely associated with the appearance of a species that absorbs at 380 nm that is referred to as metarhodopsin II (MII) (*2*).

The nature of the protein conformational change associated with receptor activation lies at the heart of the signal transduction mechanism and has been the subject of active investigation. Proteolysis (*3*), Fourier transform infrared difference spectroscopy (FTIR) (*4*), linear and circular dichroism (*5*), and cyanogen bromide reactivity (*6*) all reveal differences between native rhodopsin and the MII state as defined by the 380-nm absorbance. However, this absorbance may not uniquely define a protein conformation, and it is important to obtain direct time-resolved data on the protein conformation to draw unambiguous correlations with receptor activation and the optical transitions. In addition, it is necessary to localize the changes within the protein structure for a meaningful interpretation. To date, FTIR spectroscopy has provided the most detailed information on the conformational transitions but has not been time-resolved in the appropriate range, and the changes have only been generally localized within the structure (*4*).

In this report, we show that the time-resolved electron paramagnetic resonance (EPR) signal from spin-labeled rhodopsin in the native disc membrane directly reveals a light-triggered conformation transition in the region of the second cytoplasmic loop with an appearance rate constant and acti-

Z. T. Farahbakhsh and W. L. Hubbell, Jules Stein Eye Institute and Department of Chemistry and Biochemistry, University of California, Los Angeles, CA 90024–7008.
K. Hideg, Central Research Laboratory, Chemistry, University of Pécs, H-7643 Pécs, Hungary.

*To whom correspondence should be addressed.

vation energy similar to those of the MII intermediate. This new conformation is transient and relaxes to a rhodopsin-like state with a time course similar to the formation of MIII.

Although the structure of rhodopsin is not known, compelling evidence indicates that it, like bacteriorhodopsin, consists of seven transmembrane helical segments (*7, 8*). A secondary structural model similar to others previously reported (*9–11*) is shown in Fig. 1. The molecule contains two cysteine residues on the cytoplasmic domain, Cys^{140} and Cys^{316}, that can react readily with reagents that attack S-H groups. Because of the different reactivities of these groups, they can be individually modified with spin label methanethiosulfonate derivatives (I) and (II) to give a disulfide-linked nitroxide (*10, 12*). Chemical modification of these cysteines does not inhibit G protein activation (*13*).

The spectra of (I) selectively attached to Cys^{140} or Cys^{316} are shown in Fig. 2, A and B, respectively.

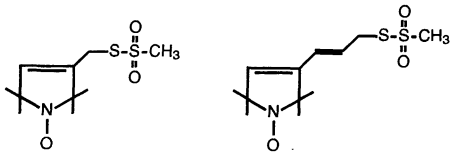

(I) (II)

In both cases, the spectra contain two major resolved components, identified as α and β, arising from relatively immobile and mobile components, respectively. Similar two-component spectra have been observed in spin-labeled proteins and were analyzed in detail for the case of hemoglobin, in which they were shown to arise from two distinct conformations of the spin label (*14*). In one conformation, the nitroxide is in direct van der Waals interaction with the protein and in slow motion, whereas in the other the nitroxide moves rapidly relative to the protein. The two motional states of (I) on rhodopsin are assumed to arise by a similar mechanism.

The model in Fig. 1 places both Cys^{140} and Cys^{316} in interhelical connecting loops at the cytoplasmic surface of the protein. This placement is supported by the high collision rates of (I) at both sites with Cr(III) oxalate (CrOx) and O_2, which indicates the exposure of those sites to the aqueous medium (*15*). Further characterization of the molecular environment is provided by spin label (II) (*16*), which is similar to (I) except for a rigid extention of the nitroxide by ~3 Å from the attachment point. This labeling resulted in a large relative increase in the mobile population β at C140, suggesting that the nitroxide-protein interaction that gives rise to the immobile population is very localized (Fig. 2C).

Photoexcitation of labeled rhodopsin produced a significant change in the relative populations of the two conformations of (I) at Cys^{140} (Fig. 2A), signaling a structural change in the protein. Apparently the changes are not global, because little change was detected at Cys^{316} (Fig. 2B) or at Cys^{222} as shown in an earlier study (*17*). The magnitude of the conformational change in the protein responsible for the spectral change at Cys^{140} is likely to be small. This likelihood is suggested by two lines of evidence. First, the change was not detected by another sensitive indicator of local conformation, namely the collision rate of the attached nitroxide with diffusible paramagnetic reagents in solution such as

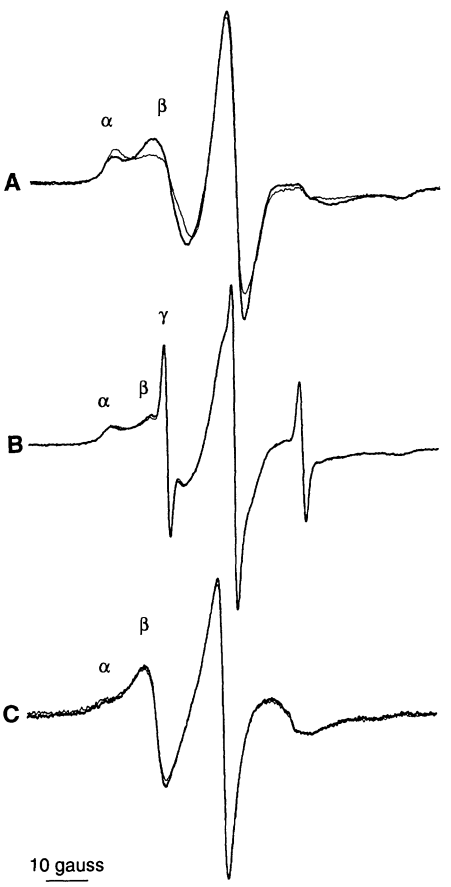

Fig. 2. The EPR spectra of spin-labeled rhodopsin recorded in the dark (thick traces) and within 30 s after 500-nm bleaching at 4°C (thin traces): (**A**) Cys^{140} labeled with (I); (**B**) Cys^{316} labeled with (I); and (**C**) Cys^{140} labeled with (II). The signal γ in (B) is due to a small amount of unattached spin label. To label Cys^{140} selectively, the more reactive Cys^{316} was blocked with 4,4′-dithiopyridine according to (*10, 12*), and Cys^{140} was then labeled with spin label (I) or (II). For specific labeling of Cys^{316}, it was first protected with 4,4′-dithiopyridine, Cys^{140} was then blocked with *N*-ethyl maleimide, and Cys^{316} was deprotected with dithiothreitol and modified with methanethiosulfonate spin label (I) or (II). Localization of the spin label at either position was confirmed by proteolytic cleavage of labeled rhodopsin with thermolysin according to (*17, 18*). In each case, >80% of the spin label was associated with either Cys^{140} or Cys^{316}.

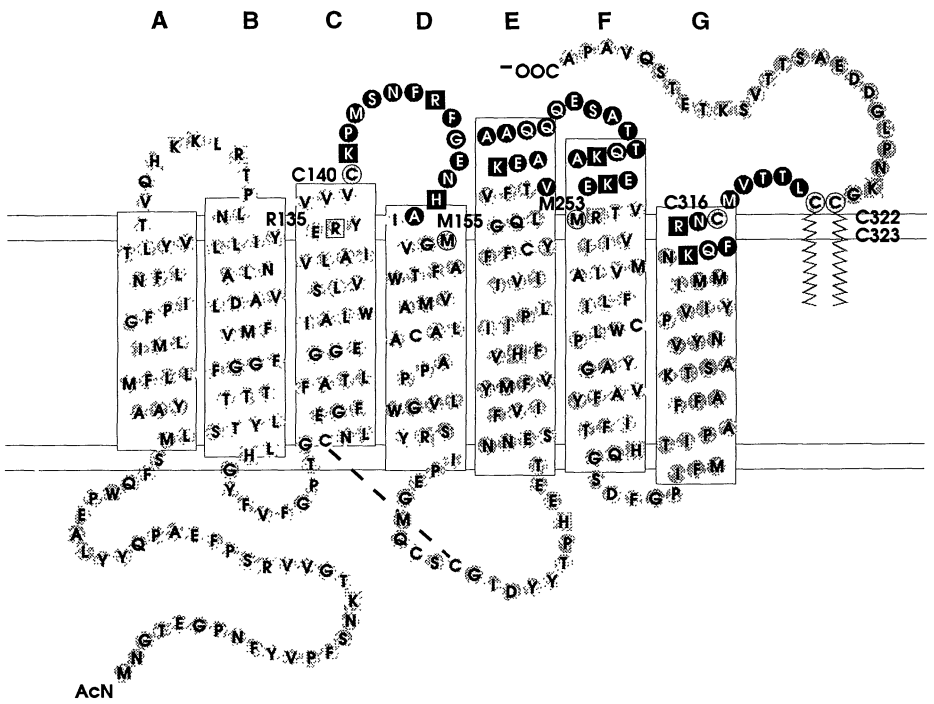

Fig. 1. A secondary structure model of rhodopsin (*30*). The position of the disulfide bond between Cys^{110} and Cys^{187} is shown as a dashed line and the palmitoylated residues (Cys^{322} and Cys^{323}) are indicated. Regions of cytoplasmic loops believed to interact with transducin according to (*4, 22*) are shown as solid symbols and various residues discussed in the text are indicated.

CrOx or O_2 (*15*). Second, previous attempts at detecting the conformational change with maleimide spin labels at Cys^{140} and Cys^{316} failed (*18*), and label (II), with a 3 Å extension of the nitroxide from the backbone, failed to detect the change. The EPR spectral change is in fact similar to that seen in the oxy to deoxy hemoglobin transition, which involves protein movement on the order of an angstrom or two (*14*). Does the conformational change detected at Cys^{140} occur rapidly enough to be involved in transducin activation, and does it correspond to the formation of a known optically detected intermediate? To answer these questions, we determined the time course of the spectral change by fixing the magnetic field at either position α or β and recording the spectral intensity after a brief flash of light. Time recordings at β after a single flash of light are shown in Fig. 3 superimposed on the optical density changes recorded at 380 nm from an identical sample. The close correspondence of the optical and EPR signal changes at various temperatures indicates that both the activation enthalpies and entropies for the processes are similar. Time recordings made at point α gave the same time course to those from β. These results directly demonstrate a movement of the protein in the vicinity of the second cytoplasmic loop with a time constant corresponding to the appearance of the 380-nm signal.

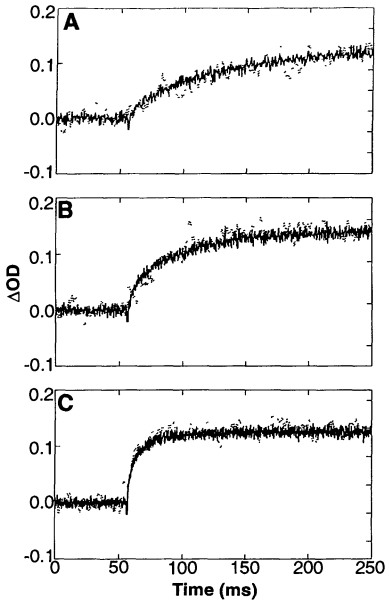

Fig. 3. Time-resolved changes in EPR spectra of spin-labeled rhodopsin (Cys^{140}) at different temperatures: (**A**) 5°C, (**B**) 9°C, and (**C**) 16°C. The magnetic field was fixed at position β as shown in Fig. 2. The change in amplitude of peak β was monitored after rhodopsin was illuminated with a xenon flash lamp with a pulse duration of 600 μs (dotted traces). The spectrometer time constant was ~1 ms. The flash lamp was equipped with a heat filter and a 500-nm-long wave pass interference filter (03 FIB 005, Melles Griot, Irvine, California). The optical density (OD) at 380 nm was monitored under the same conditions and superimposed on the EPR changes (solid traces). The EPR signal intensity was inverted and normalized in amplitude to the optical changes for comparison.

For the data in Fig. 3, the optical recordings were made with the same spin-labeled rhodopsin sample used for the EPR. A comparison of the time course for the appearance of the 380 species for labeled versus unlabeled rhodopsin reveals that the presence of the spin label at position Cys^{140} increases the formation rate of the MII species by about a factor of 2 at 15°C. This result further emphasizes that Cys^{140} is in a sensitive region of the molecule where changes occur during photoactivation. A spin label at Cys^{316} has no effect on the kinetics of MII appearance, consistent with little detected change in line shape upon bleaching.

If the time dependence of the EPR spectrum is followed for a longer period, it can be seen to relax to a line shape similar to, but not identical with, that before photoexcitation with a half time of ~6 min at 25°C (Fig. 4). This value is approximately the half time for the decay of MII to the MIII intermediate detected optically and suggests that the light-induced conformation change is reversed in this transition. This reversal is entirely consistent with a number of changes that accompany the decay of MII. In particular, MIII cannot activate transducin (*19*) and has a proteolytic cleavage pattern and rate more similar to rhodopsin than to MII (*3*). Studies with FTIR also have found that changes induced at MII reverse on passing to MIII, suggesting that the changes detected are part of the same process producing the spin label changes (*4, 20*).

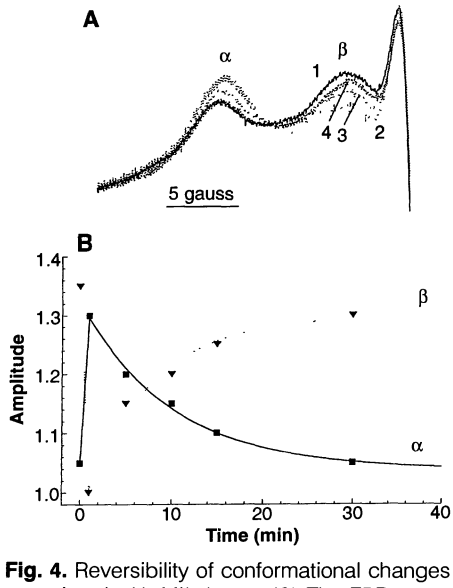

Fig. 4. Reversibility of conformational changes associated with MII decay. (**A**) The EPR spectrum 1 is obtained before illumination. Spectra 2 to 4 were obtained after 1, 5, and 15 min after illumination, respectively. (**B**) The decrease in amplitude of peak (α) and increase in amplitude of peak (β) plotted against time. The solid lines are least-squares best fit to a single exponential with a time constant of ~6 min.

The conformational change reported here is detected at the cytoplasmic surface of the rhodopsin molecule in the region of the connecting loop between helices C and D. This domain has been identified as involved in the binding, activation, or both of transducin (*21, 22*). Proteolytic cleavage studies (*3*) have localized unidentified changes in the C-D loop with light activation, and CNBr reactivity is altered at Met^{155} in helix D (*6*). Recent FTIR studies have been interpreted to show a change in an arginine residue with activation, which has been speculated to be the critical, highly conserved Arg^{135} at the base of the C-D loop (*4*). These regions are highlighted in Fig. 1 and emphasize the concentration of charges near the C-D interhelical loop domain.

What kind of conformational changes could account for the EPR spectral changes reported above? Because there is essentially no detectable change in secondary structure upon the formation of MII (*5*), it is reasonable to consider "rigid body" motions of the α helices of rhodopsin. Indeed, changes in the disposition of α helices are the basis for conformational changes in a number of proteins, including bacteriorhodopsin (*23*). Motion of the rhodopsin C helix, adjacent helices, or both could account for the spectral changes at Cys^{140}. Motion of the C helix upon photoexcitation might be anticipated, because this helix contains Glu^{113}, which forms a salt bridge with the protonated retinal Schiff base at Lys^{296} in helix G (*24*). Upon photoexcitation, the Schiff base deprotonates (*25*), and loss of the salt bridge could permit motion of the C helix about a fulcrum provided by the conserved 110 to 187 disulfide (Fig. 1). In fact, recent results from mutagenesis show that changes disrupting the 113 to 296 salt bridge result in the constitutive activation of the receptor (*26*), suggesting a crucial role for this salt bridge in maintaining the inactive conformation. A recent model for the organization of the rhodopsin helices places helices D, E, F, and G in close apposition to helix C (*27*). In the context of this model, the motion of any of these helices relative to C could also account for the data. However, the motion of helix G is considered less likely because spin label (I) at position 316 near the termination of that helix senses no change upon photoexcitation of the membrane-bound protein.

The origin of the conformational change can be further explored by the technique of site-directed spin labeling, in which nitroxide spin labels are selectively placed through the use of site-directed mutagenesis. With a set of spin-labeled proteins, this strategy can provide both secondary and tertiary structural information (*28*) and should permit a detailed interpretation of the conformational change observed here. The feasibility of such studies has recently been demonstrated for rhodopsin (*29*). This approach should be particularly useful for other receptors that have no natural chromophore as an indirect indicator of structural changes.

REFERENCES AND NOTES

1. T. E. Thorgeirsson, J. W. Lewis, S. E. Wallace-Williams, D. S. Kliger, *Photochem. Photobiol.* **56**, 1135 (1992).
2. K. P. Hofmann, *Photochem. Photobiophys.* **13**, 309 (1986).
3. H. Kuhn, O. Mommertz, P. A. Hargrave, *Biochim. Biophys. Acta* **679**, 95 (1982).
4. W. J. DeGrip *et al.*, *Photochem. Photobiol.* **48**, 497 (1988); U. M. Ganter, T. Charitopoulosw, N. Virmaux, F. Siebert, *ibid.* **56**, 57 (1992); A. K. Klinger and M. S. Braiman, *Biophys. J.* **63**, 1244 (1992).
5. M. Chabre, *Proc. Natl. Acad. Sci. U.S.A.* **75**, 5471 (1978); C. N. Rafferty, J. Y. Cassim, D. G. McConnell, *Biophys. Struct. Mech.* **2**, 227 (1977).
6. C. Pellicone, N. J. Cook, G. Nullans, N. Virmaux, *FEBS Lett.* **184**, 179 (1985).
7. M. Chabre, *Annu. Rev. Biophys. Chem.* **14**, 331 (1985).
8. G. F. X. Schertler, C. Villa, R. Henderson, *Nature* **362**, 770 (1993).
9. E. A. Dratz and P. A. Hargrave, *Trends Biochem. Sci.* **8**, 128 (1983).
10. J. B. C. Findlay *et al.*, *Vision Res.* **24**, 1501 (1984).
11. H. G. Khorana, *J. Biol. Chem.* **267**, 1 (1992).
12. Y. S. Chen and W. L. Hubbell, *Membr. Biochem.* **1**, 107 (1978).
13. K. P. Hofmann and J. Reichert, *J. Biol. Chem.* **260**, 7990 (1985).
14. S. Ogawa and H. M. McConnell, *Proc. Natl. Acad. Sci. U.S.A.* **58**, 19 (1967); J. K. Moffat, *J. Mol. Biol.* **55**, 135 (1971).
15. To determine the topographical location of the spin-labeled site in the molecule, the accessibility of the nitroxide to collision with CrOx and O_2 has been measured according to Farahbakhsh and colleagues [*Photochem. Photobiol.* **56**, 1019 (1992)]. The accessibility expressed as a dimensionless π value is 0.6 and 0.2 for O_2 and CrOx, respectively. These values correspond to those for solvent-exposed residues. There was no change in π after photoexcitation.
16. K. Hideg *et al.*, unpublished results.
17. Z. T. Farahbakhsh, C. Altenbach, W. L. Hubbell, *Photochem. Photobiol.* **56**, 1019 (1992).
18. M. Delmelle and N. Virmaux, *Biochim. Biophys. Acta* **464**, 370 (1977).
19. J. Kibelbek, D. C. Mitchell, J. M. Beach, B. J. Litman, *Biochemistry* **30**, 6761 (1991).
20. K. J. Rothschild, J. Gillespie, W. J. DeGrip, *Biophys. J.* **51**, 345 (1987).
21. R. R. Franke, B. König, T. P. Sakmar, H. G. Khorana, K. P. Hofmann, *Science* **250**, 123 (1990).
22. B. König *et al.*, *Proc. Natl. Acad. Sci.* **86**, 6878 (1989).
23. C. Chothia and A. M. Lesk, *Trends Biochem. Sci.* **114**, 116 (1985); C. A. McPhalen *et al.*, *J. Mol. Biol.* **227**, 197 (1992); S. Subramaniam, M. Gerstein, D. Oesterhelt, R. Henderson, *EMBO J.* **12**, 1 (1993).
24. T. P. Sakmar, R. R. Franke, H. G. Khorana, *Proc. Natl. Acad. Sci. U.S.A.* **86**, 8309 (1989); E. A. Zhukovsky and D. D. Oprian, *Science* **246**, 928 (1989).
25. E. A. Zhukovsky, P. R. Robinson, D. D. Oprian, *Biochemistry* **31**, 10400 (1992).
26. P. R. Robinson, G. B. Cohen, E. A. Zhukovsky, D. D. Oprian, *Neuron* **9**, 719 (1992); G. B. Cohen, T. Yang, P. R. Robinson, D. D. Oprian, *Biochemistry* **32**, 6111 (1993).
27. J. M. Baldwin, *EMBO J.* **12**, 1693 (1993).
28. C. Altenbach, T. Marti, H. G. Khorana, W. L. Hubbell, *Science* **248**, 1088 (1990).
29. J. Resek, Z. T. Farahbakhsh, W. L. Hubbell, H. G. Khorana, *Biochemistry*, in press.
30. Abbreviations for the amino acid residues are as follows: A, Ala; C, Cys; D, Asp; E, Glu; F, Phe; G, Gly; H, His; I, Ile; K, Lys; L, Leu; M, Met; N, Asn; P, Pro; Q, Gln; R, Arg; S, Ser; T, Thr; V, Val; W, Trp; and Y, Tyr.

31. Supported by NIH grant EY05216, NIH training grant EY07026, Hungarian Research Foundation grant OTKA/3/42, and the Jules Stein Professor Endowment.

15 July 1993; accepted 1 October 1993

Nonlinear Optical Properties of Proteins Measured by Hyper-Rayleigh Scattering in Solution

K. Clays, E. Hendrickx, M. Triest, T. Verbiest, A. Persoons,* C. Dehu, J.-L. Brédas

Hyper-Rayleigh scattering has been used to determine the nonlinear optical properties of a chromophore-containing protein in solution. Because the technique of hyper-Rayleigh scattering allows the measurement of hyperpolarizabilities in an isotropic solution without the application of an electric field, this method is ideally suited for the study of proteins that carry a net charge. The observed orientational correlation between the nonlinear optical chromophores in incompletely solubilized protein molecules suggests that guidelines from protein structures can be used for the engineering of supramolecular structures with high optical nonlinearity.

The light-energy–transducing protein bacteriorhodopsin (bR) has received considerable attention for potential application in molecular opto-electronic devices (*1–5*). The protein is present in the purple membrane (PM) of halophilic bacteria (*6, 7*). Energy production in these bacteria is based on a proton gradient established by light absorption. The light-driven proton pump action of bR is due to the retinal chromophore, which is bound to the ϵ amino group of the lysine-216 amino acid residue of the protein to form the retinylidene-*n*-butylamine Schiff base. Upon photoexcitation, the proton of the protonated Schiff base is released and follows a channel of hydrogen bonds toward the cellular exterior.

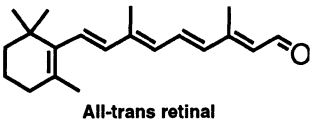

All-trans retinal

The conjugated chain in the retinal chromophore permits large odd-order electronic polarizabilities along the chain direction. In addition, the overall molecular symmetry allows second-order nonlinear optical effects. Because of the symmetry restrictions for even-order nonlinear optical effects, the direct determination of the second-order polarizability, first hyperpolarizability β, in the series expansion of the dipole moment μ_i induced by application of a strong electric field E

$$\mu_i = \alpha_{ij} \cdot E_j + \beta_{ijk} \cdot E_j E_k + \gamma_{ijkl} \cdot E_j E_k E_l + \ldots$$

can only be performed in macroscopically noncentrosymmetric ensembles. The classical experimental technique for the determination of the first hyperpolarizability of polar molecules in solution, electric-field–induced second-harmonic generation (EFISHG) (*8–10*), makes use of a dc electric field to orient the dipolar molecules. A temperature-dependent orienting of the molecules in the field then allows frequency-doubling of an intense laser pulse. Because the efficiency of frequency-doubling is dependent on the degree of dipolar orientation, the net result from an EFISHG measurement is the scalar product $\mu\beta$ of the permanent dipole moment vector μ with the vector part of the first hyperpolarizability β. Thus, the value of the dipole moment is necessary to deduce a value for β. Another possible source of error in EFISHG is the estimation of the local field factor, which accounts for the difference between the amplitude of the externally applied electric field and the actual field experienced by the molecule.

However, the EFISHG technique cannot be used with conducting solutions; thus, it cannot probe ionic materials that

K. Clays, E. Hendrickx, M. Triest, T. Verbiest, A. Persoons, Laboratory of Chemical and Biological Dynamics, Center for Research on Molecular Electronics and Photonics, University of Leuven, Celestijnenlaan 200D, B-3001 Leuven, Belgium.

C. Dehu and J.-L. Brédas, Service de Chimie des Matériaux Nouveaux, Centre de Recherche en Electronique et Photonique Moléculaire, Université de Mons-Hainaut, B-7000 Mons, Belgium.

*To whom correspondence should be addressed.